

# Economic and environmental impacts of installation of fast charging on existing buildings for V2B uses

Jae Heo<sup>1</sup>, Soowon Chang<sup>2\*</sup>

1 School of Construction Management Technology, Purdue University, 401 N. Grant St., West Lafayette, IN 47907, USA, E-mail address: [heo27@purdue.edu](mailto:heo27@purdue.edu)

2 School of Construction Management Technology, Purdue University, 401 N. Grant St., West Lafayette, IN 47907, USA, E-mail address: [chang776@purdue.edu](mailto:chang776@purdue.edu) (Corresponding Author)

## ABSTRACT

As a growing need for reducing carbon emissions, the renewable energy-based electric vehicle (EV) system has been studied. Extensive research has investigated the optimal sites for EV charging stations (EVCS) powered by photovoltaic (PV) plants. However, feasible ranges of applying EVCS powered by PV can be varied by different land use. This paper presents the effective approaches for siting and sizing EV charging stations using the geo-spatial clustering method on Geographic Information System (GIS). This study explores the optimization of site selection for charging stations depending on parcel maps and conducts an economy and environment analysis through the evaluation of potential electricity which can be generated in the study area.

**Keywords:** Electric Vehicle, Fast charging stations, Rooftop PV, Vehicle-to-building (V2B), Vehicle-to-Grid (V2G), Building category

## NONMENCLATURE

### Abbreviations

V2B	Vehicle to Building
PV	Photovoltaic
V2G	Vehicle to Grid
EV	Electric Vehicle
GHG	Greenhouse Gases
CO <sub>2</sub>	Carbon Dioxide
ICE	Internal Combustion Engine
EVCS	Electric Vehicle Charging Station
GIS	Geographic Information System
MCDCA	Multi-Criteria Decision Analysis
MINLP	Mixed-Integer Non-Linear
NAD	North American Datum
UTM	Universal Transverse Mercator
IN	Indiana state
USA	United States
DSM	Digital Surface Map
USGS	U.S. Geological Survey
TIN	Triangular Irregular Network

LASer	LAS
EPA	U.S. Environmental Protection Agency
SO <sub>2</sub>	Sulfur Dioxide
NO <sub>x</sub>	Nitric oxide and nitrogen dioxide
<i>Symbols</i>	
n	Year
DC	Direct Current
Min	Minutes
V	Volt
VA	Volt-ampere
N	North
D	Dimensional
ft	Foot
W	Watt
m	Meter
h	Hour
mi	Miles
¢	Cent
\$	Dollar
lb	pound

## 1. INTRODUCTION

Electric vehicle (EV) adoption has increased over the last 10 years, from a 0.2% share of vehicle sales in 2012 to an 8.3% EV market share in 2021 [1] in the global vehicle market. In that EVs do not emit air pollution when driving, they have been promoted for improving air quality in cities [2]. However, potential EV customers are still hesitating to adopt EVs. According to a survey conducted by consumer report, lack of public charging station is rooted as the biggest hesitation (48%) for potential EV users, followed by two disadvantages: purchase price (43%), and insufficient driving ranges (42%) [3]. Insufficient charging stations not only reduce the purchasing power of EVs but also cause a risk in which the vehicle stops while long-distance driving due to the inability to charge the vehicle.

On the other hand, EVs have been considered one of the promising technologies to reduce carbon dioxide (CO<sub>2</sub>) emissions that can cause environmental issues such as rising global temperatures and greenhouse gases (GHG). Specifically, annual emissions per vehicle by electric vehicles are around 30% less than gasoline-based internal combustion engines (ICEs). However, the CO<sub>2</sub> emissions of electric vehicles highly depend on sources of electricity, such as coal, and natural gas. For example, national averages for electricity sources are made up of natural gas of 38%; coal of 22%; nuclear of 19%; and renewables of 20% in the United States. In the state of Indiana, sources of electricity are composed of coal of 59%, natural gas of 30%, and renewables of up to 10%. Accordingly, annual emissions per electric vehicle in Indiana are two times higher than EVs that use the national average energy sources. It indicates that EV uses may not have significant impacts on carbon emissions in terms of well-to-wheel emissions, which include all emissions from the process of energy production to use.

Although extensive study of placing and sizing electric vehicle charging stations (EVCS) has been conducted to facilitate the supply of growing demand for EVs, it is still challenging that it still uses electricity produced from carbon-intensive energy sources (e.g., coals) with high CO<sub>2</sub> emissions. Thus, recent studies have designed the optimal EVCS model connecting EVCS with electricity produced from PV plants. For example, Hafez and Bhattacharya 2017 [4] proposed the optimal design of EVCS by considering physical, operating, and economic characteristics. They designed the EVCS under two different supply options: (a) isolated EVCS that directly connect to PV, and (b) grid-connected EVCS from a microgrid perspective with considering Feed-in-Tariff (FIT) to evaluate the electricity prices that paid to renewables-based energy suppliers. Shariff et al., 2020 [5] suggested the optimization design of a solar-powered EVCS in off-grid. Accordingly, the design of EVCS connected with PV plants is necessary for the site and size of EVCS and PV plants. In addition, feasible ranges of applying EVCS powered by PV can be varied by different land use [6]. To fill the gaps in the literature, this study proposes an approach for optimally selecting sites and sizing for EVCS connected with PV installed in the rooftop of buildings on a GIS environment under the microgrid concepts. The primary goals are to analyze the economic and environmental impacts of the installation of fast-charging stations by different land uses and to evaluate the capacity of EVs in the charging stations.

## 2. RESEARCH BACKGROUND

The investigation of optimal seating for the EVCS is key to expanding the spread of it for potential EV users.

Researchers have studied site selection for EVCS using a decision-making model or deep neural network model with a geographic information system (GIS). For example, Erbas et al., 2018 [7] proposed GIS-based fuzzy multi-criteria decision analysis (MCDA) to find the optimal sites of EVCS under environmental, economic, and urbanity perspectives. They found influential sub-criteria under main perspectives (e.g., EV ownership in the service area of 0.197 and distance to power cut of 0.128 under economic criteria, distance to the vegetation of 0.109 under environmental criteria, and service area population of 0.109 under urbanity criteria) for searching the areas to install the EVCS and comparing potential charging stations with current stations. Micari et al., 2017 [8] suggested a graph model-based planning of EVCS by calculating both the number and position of EVCS in a road network. They considered the EV flow and the charging station technical characteristics under different scenarios devised through changing the parameters (e.g., the autonomy of the vehicle, the safety margin, charging station power, and average energy of the battery pack).

In addition, researchers have studied the site selection of EVCS with sizing the charging station together to project the charging station investment planning as a public charging station in urban or metropolitan cities environment. Although the level 1 and level 2 charging stations are generally installed in residential (at home) or commercial (at workplace/parking lot) areas due to relatively low installation cost (~ several hundred dollars), they require to take a few hours (~4.5 hours) to fuel EVs. On the other hand, level 3 or DC-fast (called superchargers in Tesla) has strong advantages in that it relatively takes 30 min to charge EVs (filling 80% gauges). However, they are required to additionally install electronic equipment such as transformers for converting voltages (single 240V to three-phase 480V line and high current and power rating by transformer: 600 to 800 kVA), and permit from states. The fast-charging infrastructure costs up to \$60,000 [9]. Sadeghi-Barzani et al., 2014 [10] present a Mixed-Integer Non-Linear (MINLP) optimization approach for optimal site selection and sizing of the fast-charging station. They computed the total cost of charging station development including station development cost (e.g., station equipment cost and land cost) and station electrification (e.g., grid loss, EV loss), and applied its computation to the study area to find optimal sites where the total cost is minimized considering policy scenarios.

### 3. METHODOLOGY

This research explores optimal sites for installation of EVCS-powered PV power generation installed in rooftops of building at a case study in West Lafayette, IN, USA. This study also evaluated the sizing of EVCS that satisfied the optimal characteristics: the high supply of PV power generation and demand of traffic flow by geo-spatial analysis using GIS modified by a methodology presented in [11].

#### 3.1 Data collection

This study uses two spatial data types (e.g., traffic count, and PV power output). All data used for sitting and sizing the EVCS were digitalized using a uniform coordinate system (i.e., North American Datum (NAD) 1983 Universal Transverse Mercator (UTM) 16N) and the same resolution (i.e.,  $10 \times 10 \text{ ft}^2$ ). West Lafayette in Indiana, United States, was chosen as the case-study area (Fig. 1). The case study area consists of various parcels (e.g., residential, commercial, industrial/agricultural, and state/government-owned), and thus a spatial analysis is required for identifying installation sites for EVCS in each parcel region.

For representing the demand for electricity by EV users, traffic count data was collected from continuous numerical maps (e.g., polyline layers) at a fixed interval of 10 ft provided by the Indiana Department of Transportation (INDOT) [12]. These traffic count data define the average daily traffic values for the year and calculate the volumes of traffic passing both directions of the road. The traffic count data were transformed from continuous polyline layer format to discrete point layer to process the spatial autocorrelation analysis.

The PV power outputs are obtained by estimating the daily available solar irradiation at a raster level using the area solar radiation method in ArcGIS and the global formula for estimation of the electricity generated in the output of a photovoltaic system. The solar radiation analysis in ArcGIS enables to calculate the insolation

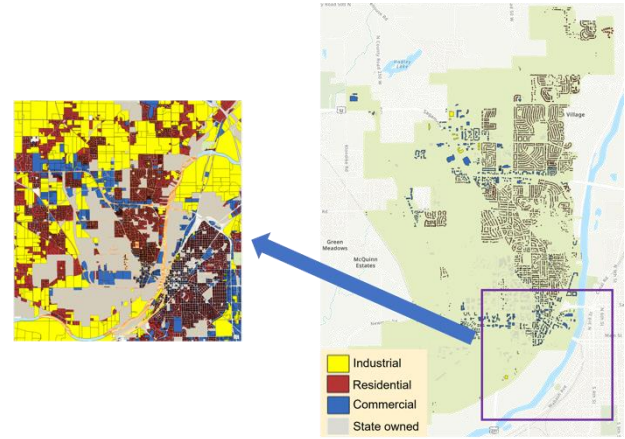


Fig. 1 The parcel maps in case study area: West Lafayette, Indiana state in United States.

across an entire map, which can consider the effects of geographical effects (i.e., shadow effect, sky view effect) on solar irradiation, using only geographic data (i.e., digital surface map, DSM) [13]. DSM, a representation of the bare ground topographic surface of the Earth including surface objects (e.g., trees, buildings) as three-dimensional (3D) elevations, was computed using a lidar point cloud map provided by U.S. Geological Survey (USGS) [14]. The DSM map can be generated through two steps as shown in Fig. 2): (a) create the triangular irregular networks (TIN) terrain map from point cloud-based elevation data in LASer (LAS) format, and (b) convert the TIN map into raster images. Creating a TIN is for interpolating the elevation values in an empty space by forming a network of triangles. Then, the TIN map was transformed into a raster image (i.e., DSM) using data conversion functions in geoprocessing tools on GIS. Finally, the DSM map was used to estimate yearly solar radiation and was extracted through a building footprint map for obtaining only the values located overlaying the building map that indicates generating the PV power output from solar PV plants installed on the rooftop of the buildings.

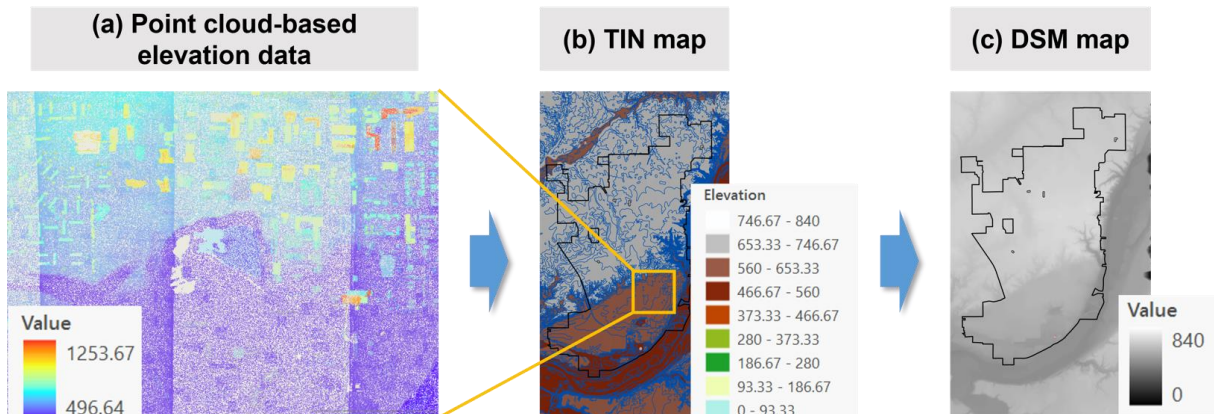


Fig 2. The process of creation of DSM map for solar irradiation generation: (1) Conversion of point cloud into TIN, and (2) Conversion of TIN into DSM.

Table 1. The results of predicted daily potential electricity.

	Solar irradiation (Wh.y)	Rooftop area (ft <sup>2</sup> )	Efficiency (%)	Yearly Energy (Wh.y)	Daily Energy (kWh.d)
Residential	$1.246 \times 10^{10}$	$1.022 \times 10^6$	18.1	$1.691 \times 10^{11}$	$4.634 \times 10^5$
Commercial	$7.553 \times 10^9$	$6.320 \times 10^5$	18.1	$1.025 \times 10^{11}$	$2.809 \times 10^5$
Industrial	$5.431 \times 10^8$	$4.445 \times 10^4$	18.1	$7.373 \times 10^9$	$2.020 \times 10^4$
State owned	$8.267 \times 10^9$	$7.132 \times 10^5$	18.1	$1.122 \times 10^{11}$	$3.075 \times 10^5$

Furthermore, based on the solar irradiation map (Wh), this paper generated the daily electricity generation from rooftop PV (Wh/day) using the Equation 1 based on [15]; where A denotes total solar panel area (m<sup>2</sup>), r denotes solar panel yield or efficiency (%) (the solar panel yield of a PV module of 200 Wp with an area of 1.1 m<sup>2</sup> is 18.1%) in Equation 2, H denotes annual average solar radiation on tilted panels, and PR denotes performance ratio, the coefficient for losses (i.e., the default value is 0.75 for the performance of installation independently of the orientation, inclination of the panel). Table 1 shows the daily PV power output at the test site represented in different parcels.

$$E \text{ (kWh)} = \frac{A \times r \times H \times PR}{365} \quad (1)$$

$$r = \frac{\text{electrical power of one solar panel}}{\text{the area of one panel}} \quad (2)$$

### 3.2 Modeling spatial weights

For suitability analysis, a spatial autocorrelation is used as the computational model that is about social or physical processes to find or cluster the similar/dissimilar to nearby sites. While the Moran's I measure how a site is apposite to its neighborhood, the Getis-Ord Gi statistics describe "how large the neighborhood of a given site is relative to the average neighborhood" in (Oxoli 2019, page 3) [16]. This analysis is used to perform evidence of spatial patterns that can be presented by the ratio of peripheral observations at site i to the sum of all observations, including those not at site i, Equation 3 based on [17]. However, the x<sub>j</sub> values are not ruled in standardized distribution, and thus it is needed to transform the raw Gi statistics to be centered on zero-as-normal distribution, the Equation 4 based on [18], for interpreting around site i of neighboring sites j within distance d (i.e., w<sub>ij</sub>).

$$G = \frac{\sum_i^N W_{ij} X_j}{\sum_i^N X_j} \quad (3)$$

$$Z_i = \frac{G_i - E[G_i]}{\sqrt{\text{Var}(G_i)}} \quad (4)$$

$$E(G_i) = \frac{\sum_i^N W_{ij}}{n(n-1)} \quad (5)$$

The G statistic can be interpreted through clustering high/low values in/around the target spot. The G index can discern cluster structures of high- or low-value concentration (e.g., traffic count, PV power output) among local observations. Overall, this study used a Getis-Ord Gi statistics-based hotspot analysis to evaluate spatial clusters of traffic count and PV power output in West Lafayette city using an ArcGIS environment. The high values in the attribute are extracted in the statistical analysis and apply these results to search for the best sites for installation of EVCS where both attributes satisfy the high values (i.e., high-high values).

### 3.3 Evaluation of economic and environmental impacts

There were over 20 EVs for sale in the United States in 2021, automakers were launching these cars with varied car specifications. In other words, it makes a difference between taking the time to charge EVs, and adding electricity for driving miles. This study determines one brand, TESLA Model 3 Saloon Long Range All-Wheel Drive (AWD) 4dr Auto, for uniformly evaluating the economy for EVs charged. This model has a relatively well specification of 358 miles range (environmental protection agency, EPA), and a 78 kWh battery size. The specification of fleets (i.e., charger power output) is used to calculate the charging time. Installing the charger power output depends on the parcel region. For example, the level 2 chargers (7kW) are installed in residential regions; two different level 3 chargers (50kW, and 150kW) are installed in industrial/agricultural, state/government, and commercial regions. Overall, to estimate the time it will take to charge an EV, the size of battery capacity in kilowatt-hours divided by the charging power times under assuming that "EVs charge up to 80% of battery capacity" and "the efficiency of the charger is 100%" as shown in Equation (6).

$$\begin{aligned} & \text{charge time (h)} \\ &= \frac{\text{battery capacity}}{\text{charge power} \times \text{power efficiency}} \end{aligned} \quad (6)$$

*Table 2. The specification of EVs in different fleet characteristics.*

	Residential (7kW)	Commercial (150kW)	Commercial (50kW)	Industrial (150kW)	Industrial (50kW)
Charging time	8.9 h	25 min	1.2 h	25 min	1.2 h
kWh added	62 kWh	62 kWh	62 kWh	62 kWh	62 kWh
Range added	288 miles	288 miles	288 miles	288 miles	288 miles
Electricity rates	10.53 ¢/kWh	9.14 ¢/kWh	9.14 ¢/kWh	6.34 ¢/kWh	6.34 ¢/kWh
Charging cost	\$ 6.82	\$ 5.75	\$ 5.75	\$ 3.95	\$ 3.95
Cost per mile	2.368 p	1.997 p	1.997 p	1.372 p	1.372 p

For example, as shown in Table 2, in a residential parcel, it takes 8.9 h to charge, which took longer than other parcels using relatively high charger power (e.g., 50 kW, 150 kW) and the cost of electricity to charge 288 miles for driven was calculated at \$6.82 applying electricity rates in IN (10.53 ¢/kWh) without the definition of a progressive tax. In commercial and industrial parcels, the charging time and charging cost were calculated under different level 3 charge power (e.g., 50 kW and 150 kW) that it took 25 min at a 150 kW and 1.2 h at a 50 kW charger, respectively. Specifically, electricity costs for state/government-owned parcels were calculated by applying industrial electricity rates.

In addition, to calculate the available number of EVs charged in each fleet, this study assumed that all EVs are charged when their battery levels are between 0% and 80%; they leave the stations after completing the charging.

This study estimates CO<sub>2</sub> emissions reduction by changing the electricity resources from generated by general methods (e.g., thermal power stations) to generated by renewable sources (e.g., solar PV plants)

during driving the EVs. The avoided CO<sub>2</sub> emissions can be calculated through the greenhouse gas equivalencies calculator presented by the United States Environmental Protection Agency (EPA) [19].

#### 4. RESULT

##### 4.1 Spatial weight evaluation

Table 3 provides the information on the spatial relationships among the spatial features (e.g., traffic count, PV power output) using P-value and Z-score. It further provides analysis according to different parcel regions (e.g., commercial, industrial/agricultural, state/government-owned sites) except for residential regions where one charger is installed to one house without the need to charge EVs quickly. As a result, the P-values were less than 0.05 in both cluster analysis of traffic count and PV power output with two parcel regions: commercial and state-owned regions. The null hypothesis can be rejected; and the spatial patterns are clustered in specific spots (i.e., not random processes). In addition, the spatial distribution of high values can be clustered when the observed general G index is greater

*Table 3. The spatial relationships among the spatial features.*

Parcel regions	Analysis type	Observed General G	Expected General G	Z score	P value	Pattern
State owned	PV power output	0.00181	0.00180	2.255	0.024	High-Clusters
	Traffic count	0.00109	0.000067	35.434	< 0.01	High-Clusters
Commercial	PV power output	0.01295	0.01294	2.809	0.005	High-Clusters
	Traffic count	0.00074	0.00044	56.568	< 0.01	High-Clusters
Industrial	PV power output	0.03570	0.03570	-0.251	0.802	Random
	Traffic count	0.02660	0.20000	6.199	< 0.01	High-Clusters
Entire region	PV power output	0.00167	0.00167	8.85	< 0.01	High-Clusters
	Traffic count	0.000241	0.000152	77.711	< 0.01	High-Clusters

than the expected general G index with a positive Z-score in all parcels. In this respect, we exclude industrial parcels from the analysis.

accommodating relatively many fleets in state-owned areas (Fig. 3b and Table 4).

Furthermore, on the commercial parcel, the new

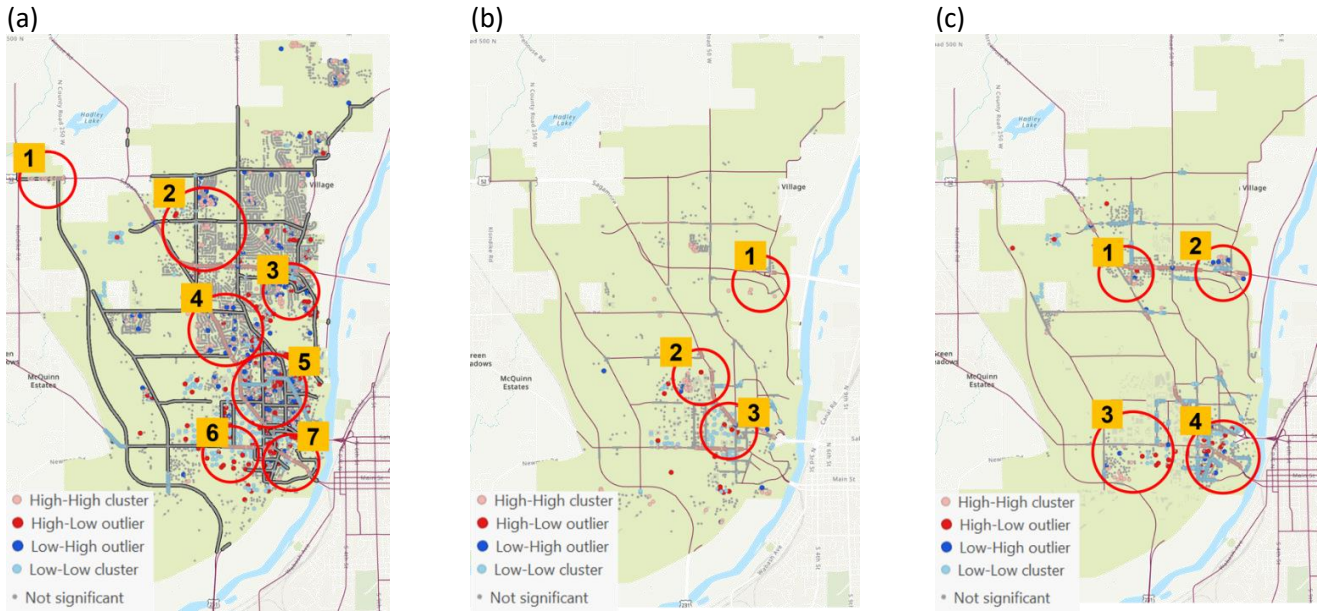


Fig. 3 EVCS site selections: (a) Suitable sites for EVCS powered by rooftop PV; (b) EVCS in state-owned areas; and (c) EVCS in commercial areas

#### 4.2 Site selection of EVCS

The potential sites of EVCS with high or low values were determined in the local spatial autocorrelation analysis using High/Low clustering (Getis-Ori General G), and Cluster and Outlier Analysis (Anselin Local Moran's I). Fig. 3 illustrates the overall clusters of solar power output produced in rooftop PV as a supply aspect and of traffic count as a demand aspect.

In particular, clustering analysis is shown by classifying five classes from a high-high cluster (i.e., a high value of PV power output or heavy traffic flow clustered) as pink color to a low-low cluster (i.e., a low value clustered) as sky blue color with not significant clustered as gray color. This study determines optimal sites under two strategies: (a) where both PV power output and traffic count are very high, which are sites 1, 2, 3, and 4 in Fig. 3a, and (b) traffic flow is very high compared to other regions, as shown in site 5 in Fig. 3a. To be specific, at the fifth candidate site, PV power output was relatively insufficient for providing electricity so that connecting with neighboring rooftop PV will be needed.

The hotspot cluster map was further analyzed to determine the installation of EVCS at appropriate sites in different parcel regions. On the state-owned parcel, the new charging stations would be intensively installed at sites 1 and 2, as shown in Fig. 3b. It implies that a small number of charging stations should be planned for

charging stations would be installed where inter-city travel occurs (sites 2 and 4), the northern part of the city (site 2), and the university airport (site 3) in Fig. 3c. EVCS installation strategy for commercial parcels would be established that fleets are dispersed to many charging stations (Fig. 3c and Table 4).

#### 4.3 Sizing of charging station and counting of the capacity of EVs in EVCS

Based on the prediction of daily potential electricity in section 2.1 and the assumption of EVs and fleets in section 2.3, we calculated the daily capacity of EVs and the installation of the number of fleets in each parcel (Table 4). In particular, to calculate the daily capacity of EVs, the EV battery capacity (80%, 62.4kWh) was divided into potentially productive electricity (daily energy in table). Based on the number of EVs, we calculated the available installation of the number of fleets that (a) the maximum acceptable EV per fleet (daily unit) was calculated by dividing 24 hours into charging time per single EV, and (b) the total number of fleets was calculated by dividing the total number of EVs into the maximum acceptable EV per fleet in two different charging speed (e.g., 50kW, 150kW). In residential parcels, the number of fleets or EVs was calculated as the number of houses where rooftop PV can be installed since the residential area installs one fleet per house.

*Table 4. The capacity of EVs under potential electricity production by rooftop PV in the test area and the number of fleets for each parcel's EVCS in different charging speeds (e.g., 50 kW, 150 kW)*

Parcels	The number of EVs	The number of fleets	
		Charging speed	
		50 kW	150 kW
Residential	(i.e., the number of houses)	4623	
Commercial		47	226
Industrial	326	3	16
State-owned	4960	51	247

#### 4.4 Reduction-effectiveness of CO<sub>2</sub> emissions

The evaluation of daily potential electricity from rooftop PV was analyzed to identify how much tailpipe emissions can be reduced by replacing the energy sources from coal-based production with solar energy for driving the EVs. In this study, four different parcel regions, residential, commercial, industrial, and state-owned (Table 5), were compared in terms of three types of tailpipe emissions; CO<sub>2</sub>, SO<sub>2</sub>, and NO<sub>x</sub>. Overall, it showed the largest tailpipe reduction (CO<sub>2</sub> of -19,820 tons; SO<sub>2</sub> of -14.645 tons; and NO<sub>x</sub> of 12.745 tons) in residential regions where the most electricity could be produced by rooftop PV. Tailpipe emissions can be decreased through the replacement of electrical energy sources, in addition to the tailpipe reduction effect while driving the EVs.

*Table 5. Reduction of environmental emissions by installing EVCS-powered by rooftop PV*

Parcels	CO <sub>2</sub> (tons)	SO <sub>2</sub> (lb)	NO <sub>x</sub> (lb)
Residential	-19,820	-29,290	-25,490
Commercial	-13,820	-20,890	-18,290
Industrial	-860	-1,280	-1,110
State owned	-19,440	-16,920	-13,160

## 5. DISCUSSION AND CONCLUSIONS

This study suggests a geospatial analysis-based investigation of optimal sites for the installation of EVCS connecting with the rooftop PV. The optimal sites are determined through satisfying the conditions of both the PV power output and traffic flow. The result discovered that searching for optimal sites is heavily influenced by parcel areas (e.g., residential, commercial, industrial, state-owned). For example, in the entire region (Fig. 3a) and commercial region (Fig. 3c), we could find the optimal sites using clustering analysis where both two factors were high. On the other hand, in the state-owned area, it was relatively difficult to find an area that met both factors.

In addition, the estimation of sizing the EVCS, proposed in previous studies, has focused on building the optimal design of EVCS when they connect with PV plants. On the other hand, we can devise a plan for determining how many fleets are installed in charging stations (Table 4). These results help to evaluate the project economy for the management of charging stations and to solve the problem of demand for charging stations due to the expansion of EV supply. Furthermore, this study may contribute to reducing carbon dioxide while driving EVs by replacing the electric energy sources from coal and natural gas with solar energy.

However, the proposed approach cannot implement the scheduling of electricity charging to EVs and supply from PV plants at a fine temporal resolution (e.g., hourly), which can be used to evaluate energy flow for the management of EVCS accurately. Thus, future work has to expand the current approach by considering the scheduling of charging patterns and applying it to other areas that can present complex parcel areas to generalize our approach.

## ACKNOWLEDGEMENT

This research was partially supported by the seed grant funding of the Future Work and Learning (FWL) Research Impact Area by Office of Research in Polytechnic Institute, Purdue University.

## REFERENCE

- [1] Irle R. EV-Volumes - The Electric Vehicle World Sales Database 2021. <https://www.ev-volumes.com/> (accessed May 6, 2022).
- [2] Hu X, Chen N, Wu N, Yin B. The Potential Impacts of Electric Vehicles on Urban Air Quality in Shanghai City. *Sustainability* 2021;13:496. <https://doi.org/10.3390/su13020496>.
- [3] Consumer Reports. Consumer Interest and Knowledge of Electric Vehicles 2020 Survey Results 2020.
- [4] Hafez O, Bhattacharya K. Optimal design of electric vehicle charging stations considering various energy resources. *Renew Energy* 2017;107:576–89. <https://doi.org/10.1016/j.renene.2017.01.066>.
- [5] Shariff SM, Alam MS, Ahmad F, Rafat Y, Asghar MSJ, Khan S. System Design and Realization of a Solar-Powered Electric Vehicle Charging Station. *IEEE Syst J* 2020;14:2748–58. <https://doi.org/10.1109/JSYST.2019.2931880>.
- [6] Chang S, Cho J, Heo J, Kang J, Kobashi T. Energy infrastructure transitions with PV and EV combined systems using techno-economic analyses for decarbonization in cities. *Appl Energy*

- 2022;319:119254.  
<https://doi.org/10.1016/j.apenergy.2022.119254>.
- [7] Erbaş M, Kabak M, Özceylan E, Çetinkaya C. Optimal siting of electric vehicle charging stations: A GIS-based fuzzy Multi-Criteria Decision Analysis. *Energy* 2018;163:1017–31. <https://doi.org/10.1016/j.energy.2018.08.140>.
- [8] Micari S, Polimeni A, Napoli G, Andaloro L, Antonucci V. Electric vehicle charging infrastructure planning in a road network. *Renew Sustain Energy Rev* 2017;80:98–108. <https://doi.org/10.1016/j.rser.2017.05.022>.
- [9] DiNello S. How Much Do EV Charging Stations Cost? *Future Energy* 2021. <https://futureenergy.com/how-much-do-ev-charging-stations-cost/> (accessed May 26, 2022).
- [10] Sadeghi-Barzani P, Rajabi-Ghahnavieh A, Kazemi-Karegar H. Optimal fast charging station placing and sizing. *Appl Energy* 2014;125:289–99. <https://doi.org/10.1016/j.apenergy.2014.03.077>.
- [11] Heo J, Chang S. Optimal installation of electric vehicle charging stations connected with rooftop photovoltaic (PV) systems: a case study, Las Vegas, NV, USA: March 2022., Accepted.
- [12] U.S. Indiana Department of Transportation (INDOT). Traffic Count Database System (TCDS) 2022., <https://indot.public.ms2soft.com/tcds/tsearch.asp?loc=Indot&mod> (accessed May 22, 2022).
- [13] ESRI. Area Solar Radiation (Spatial Analyst)—ArcGIS Pro | Documentation May 2021. <https://pro.arcgis.com/en/pro-app/2.8/tool-reference/spatial-analyst/area-solar-radiation.htm> (accessed May 26, 2022).
- [14] U.S. Geological Survey. About 3DEP Products & Services January 2022. <https://www.usgs.gov/3d-elevation-program/about-3dep-products-services> (accessed May 26, 2022).
- [15] Šúri M, Huld TA, Dunlop ED. PV-GIS: a web-based solar radiation database for the calculation of PV potential in Europe. *Int J Sustain Energy* 2005;24:55–67. <https://doi.org/10.1080/14786450512331329556>.
- [16] Oxoli D. Exploratory approaches in spatial association analysis: Methods, complements, and open GIS tools development. Polytechnic University of Milan, 2019. <https://doi.org/10.13140/RG.2.2.28112.53761>.
- [17] Hot Spot Analysis (Getis-Ord  $G_i^*$ ) (Spatial Statistics)—ArcGIS Pro | Documentation May 2021. <https://pro.arcgis.com/en/pro-app/2.8/tool-reference/spatial-statistics/hot-spot-analysis.htm> (accessed May 26, 2022).
- [18] What is a z-score? What is a p-value?—ArcGIS Pro | Documentation May 2021. <https://pro.arcgis.com/en/pro-app/2.8/tool-reference/spatial-statistics/what-is-a-z-score-what-is-a-p-value.htm> (accessed May 26, 2022).
- [19] United States Environmental Protection Agency (EPA). AVERT Web Edition | US EPA March 2022. <https://www.epa.gov/avert/avert-web-edition> (accessed May 22, 2022).